Journal of Ceramic Processing Research. Vol. 18, No. 2, pp. 108~111 (2017)

J O U R N A L O F
Ceramic Processing Research

Facile fabrication of SnS microflower-graphene with efficient photocatalytic activity under visible light

Zeng Bin[a,b] and Yang Yin[a,*]

[a]*Hunan Collaborative innovation Center for construction and development of Dongting Lake Ecological Economic Zone, Changde 415000, People's China*

[b]*College of Mechanical Engineering, Hunan University of Arts and Science, Changde 415000, People's China*

SnS microflower-graphene (G-SnS) has been successfully prepared by microwave method. Scanning electron microscopy and transmission electron microscopy observations confirm that flower-like SnS composing of numerous nanoplates as building blocks are homogeneously attached onto the surface of graphene. The experimental results show that these nanocomposites have high visible-light photocatalytic activities towards methyl orange (MO). It is believed that the hierarchical nature of the microflower structure and the intimate combination of microflower with graphene are responsible for the enhanced photocatalytic performance.

Key words: Graphene, SnS microflower, Photocatalytic performance.

Introduction

The assembly of different nanostructured building blocks into one larger configuration has received much attention in recent years [1]. Usually, hierarchical configurations are composed by nanoparticles [2], nanorods [3] or nanoplates [4]. In contrast to counterpart nanoparticles or nanorods, nanoplates have larger specific surface area, stronger light absorption capability and faster electron transport ability [5]. So the hierarchical organizations composed by nanoplates have great potential for applications in many fields.

With a 2D layer structure of sp2-hybridized carbon atoms, graphene has an effectively zero conduction resistance for transporting electrons and possess potentially electron transport capability [6]. It has been demonstrated that assembling hierarchical structure together with graphene can provide an improved charge transport and further inhibit the recombination of electron-hole pairs [7]. Until now, some progresses of graphene-hierarchical organization have been achieved. For examples, Sun *et al.* fabricated three-dimentional flower-like hetero-structured C_3N_4/SnS_2/graphene composites by a facile solvothermal method and the results showed that the composites exhibited enhanced activities in the photo-catalytic reduction of aqueous Cr(VI) [8]. Liu et al. prepared CuO nanoflower-decorated graphene nano-composites and the resulting nanocomposites can serve as an effective photocatalyst for degradation of rhodamine B [9]. Lui et al. developed graphene-TiO_2 nanoflower using the hydrothermal method and the composite has a higher photocatalytic performance than that of commercial P25 [10]. However, to the best of our knowledge, graphene-SnS flower-like structures have not been reported.

Herein, we successfully synthesized graphene decorated with SnS microflowers by the microwave assisted method. These nanocomposites show the high visible-light photocatalytic activities towards MO dye degradation. A possible photocatalytic mechanism of the hybrids was also discussed.

Experimental Details

The synthesis of SnS microflower-graphene was as follows: 1.2 g of Tin (II) chloride dihydrate ($SnCl_2$) were dissolved into 30 ml of glycol and sonicated for 30 min. Then a certain of graphene oxides (GO) powder was mixed with the prepared solution. Subsequently, 0.7 g of thioacetamide (TAA) and 0.5 g of Polyvinyl Pyrrolidone (PVP) was added. After vigorous stirring for 30 min the suspension was heated for 30 min in the microwave and the grey precipitation was produced. Then the precipitates were collected by a centrifuge with ethanol. At last, the precipitates were dried in a vacuum oven at 60 ºC overnight. For comparison, the amount of GO was varied as 1 wt%, 2 wt% and 3 wt% and the prepared samples were labeled as SnS-G1, SnS-G2, SnS-G3.

The morphology of SnS-G was observed by scanning electron microscope (SEM, S4800) and a transmission electron microscope (TEM, JEM-2100F) respectively.

*Corresponding author:
Tel : +15973622694
Fax: +086-0736-6624382
E-mail: 240939138@qq.com

The crystal structures of SnS-G were characterized by X-ray diffraction (XRD, D5000) with Cu Kα radiation. The Fourier transform infrared spectra (FTIR) were obtained under a infrared spectrometer (FTIR, WQF-410). Raman spectra was conducted using Raman spectrometer (J-Y, T6400). The EIS measurements were performed on a CHI660B workstation by using three-electrode cells according to the reference [11].

The photoefficiency of the synthesized catalysts was measured toward degradation of MO solution under visible light irradiation. 20 mg as-products were dispersed in 300 mL MO solution of 20 mg L^{-1}. After stirring for 30 min in darkness to reach adsorption desorption equilibrium, the solutions were exposed to visible light irradiation. At 30 min interval 5 mL portion was then withdrawn and separated to remove the suspended solid. The absorbance of the clean solutions at 464 nm was determined by UV-vis spectrophotometry.

Results and Discussion

The composed phases of the SnS-G2 nanocomposites are characterized by the XRD. As shown in Fig. 1(a), an obvious diffraction appears at about 25 ° can be indexed to the disorderedly stacked graphene sheets and all the other peaks can be well matched to the orthorhombic SnS phase (JCPDS card No: 39-354). No other characteristic peaks were observed, indicating the high purity of the obtained products.

Fig. 2(b) depicts the FTIR spectrum of GO and SnS-G2. The peaks of GO at 1074 cm^{-1}, 1375 cm^{-1}, 1620 cm^{-1}, 1720 cm^{-1} and 3403 cm^{-1} were assigned to oxygen-containing functional groups, i.e., C-O stretching vibrations, carboxyl O-H stretching vibrations, H-O-H stretching vibrations, C = O carbonyl stretching vibrations and H-O stretching vibrations, respectively. In the spectrum of SnS-G2 the intensities of characteristic absorption bands decreased dramatically compared with the ones of GO, indicating that SnS-G2 has less oxygen-containing groups on its surface and an obvious reduction of GO by the microwave process has been realized. This guarantees the efficient electron transport in the nanocomposites [11].

Raman measurement is an effective way to determine the surface microstructure of carbon-based materials. Fig. 1(c) shows the Raman spectroscopy of GO and SnS-G2 nanocomposites. Two obvious prominent bands D (1352 cm^{-1}) and G (1613 cm^{-1}) arising from the breathing mode of κ-point phonons of A_{1g} symmetry and E_{2g} phonons of sp2 C atoms can be clear seen. The values of the D/G intensity ratio (I_D/I_G) for GO is about 1.12, while the I_D/I_G of SnS-G2 is about 1.21, deducing the result of the reduction of the sp2 network of GO after the microwave process [12].

Fig. 1(d) shows the impedance plots of the nano-composites. It can be seen that SnS-G had smaller radius than those of the pure SnS electrode and with increasing the content of graphene in the composites, an obviously smaller radius can also be obtained. The smaller radius correspond a higher conductivity, resulting a lower resistance of the interfacial charge transfer between graphene and SnS. It means that an effectively decreased recombination of electrons-holes in the nanocomposites has been realized [13].

The information of morphology is examined by SEM, TEM and HR-TEM. From the SEM images of SnS-G2 composite (Fig. 2(a)), it is clearly seen that the flower-like SnS composing of many plates are homogeneously attached onto the surface of graphene. Additionally, for the graphene 2D transparent sheets structure with observable presence of ripples (as arrows in Fig. 2(a)) can be clear seen which means that the restacking phenomenon of graphene in the composites has been improved greatly, suggesting that the microflowers can act as spacers to prevent graphene sheets restacking.

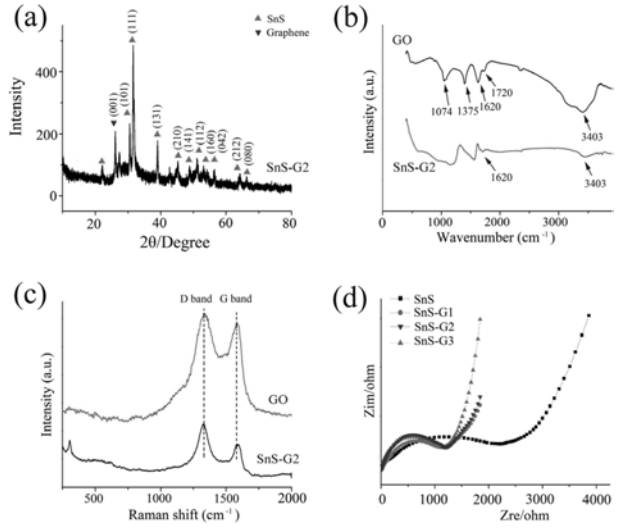

Fig. 1. (a) XRD, (b) FTIR, (c) Raman spectrum, (d) EIS spectrum of the nanocompsites.

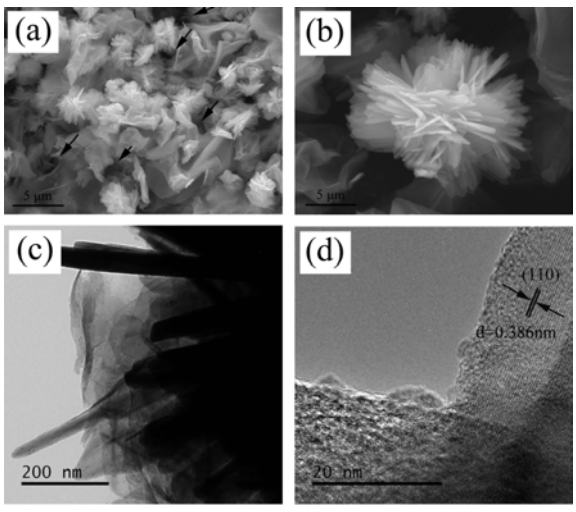

Fig. 2. (a, b) SEM, (c) TEM, (d) HR-TEM of the SnS-G2 nanocomposites.

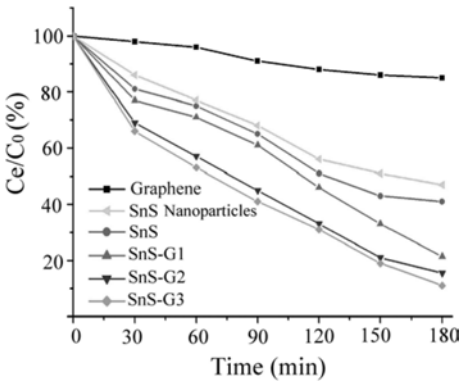

Fig. 3. Photocatalytic degradation efficiency of MO with different catalysts under visible light.

From the high-magnification SEM (Fig. 2(b)), the hierarchical SnS are well assembled by radial-aligned lamellar and form a three-dimensional flower-like structure with micrometer scale. Fig. 2(c) is a typical TEM image of the nanocomposite. It can be seen that the building blocks grow along the radial direction. The lattice spaces of 0.386 nm in HR-TEM image (Fig. 2(d)) could be indexed as (110) plane of SnS.

The photocatalytic activities of the samples are investigated under visible light irradiation. As shown in Fig. 3, pure graphene hardly degraded the MO molecules and SnS nanoparticles could degrade MO to some extent. When SnS microflowers are formed, an enhanced photocataltyic performance can be seen, indicating hierarchical nature of the microflower structures are beneficial for the photocatalytic performance. With the introduction of graphene, the obvious enhancement of photocataltyic efficiency could be seen. The data demonstrated that SnS-G2 composite possessed the best photocatalytic activity.

The photocatalytic mechanism is summarized in Scheme 1. With a narrow band gap energy (1.81 eV) of SnS, the electrons at the valence band (VB) are excited to the conduction band by visible light ($\lambda > 420$ nm), inducing the generation of photoelectrons and holes pairs [14]. Subsequently the photoinduced electrons are transferred from SnS to graphene and then the photo-generated electrons were lively to take part in to form radicals which can induce the degradation of organic dyes (MO) effectively [15]. The reason that SnS-G has a superior photocatalytic performance is as follows. Firstly, SnS microflowers composed by nanoplates have larger specific surface area, stronger light absorption capability and faster electron transport ability. The integrated properties of microflowers could exhibit excellent pollution cleanup ability [16]; Secondly, when SnS are archored onto the surface of conductive graphene, graphene serve as an acceptor of the photoexcited electrons and effectively suppress the charge recombination, thus improving the photocatalytic activity [17].

Conclusions

The graphene loaded flower-like SnS were prepared via microwave method. The prepared SnS-G hybrid material showed a high photocatalytic efficiency. It is attributed to the hierarchical nature of the microflower structure and the intimate combination of microflower with graphene. Our approach offers a new method for the large scale, low-cost production of high performance photocatalyst

Acknowledgments

This work was supported by the Natural Science Foundation of China (NSFC, No. 50972043), the Construct Program of the Key Discipline in Hunan Province and Project of Hunan Provincial Education Department (15B158).

References

1. J. Bu, J. Fang, W.R. Leow, et al., RSC Adv. 5 (2015) 203895-103900.
2. Z.L. Zhang, H.W. Che, Y.L. Wang, et al., Ind. Eng. Chem. Res. 51 (2012) 1264-1274.
3. F. Huang, W. Yang, F. He, et al., Sensors Actuat. B: Chem. 235 (2016) 86-93.
4. Y. Zhu, N. Sun, W. Lin, et al., RSC Adv. 5 (2015) 68061-68066.
5. H. Zhong, G. Yang, H. Song, et al., J. Phys. Chem. C

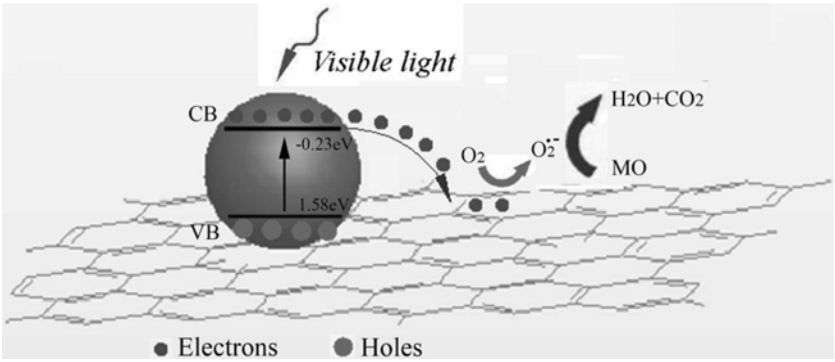

Scheme 1. Proposed photocatalytic mechanism of SnS-G composites.

116[16] (2012) 9319-9326.
6. R.E. Pearce, V. Eless, A. Lartsev, et al., Carbon 93 (2015) 896-902.
7. B. Zeng and H. Long, Nano 9 (2014) 1450097.
8. M. Sun, Q. Yan, T. Yan, et al., RSC. Adv. 4 (2014) 31019-31027.
9. S. Liu, J.Q. Tian, L. Wang, et al., Catal. Sci. Technol. 2 (2012) 339-344.
10. G. Lui, J.Y. Liao, A.S. Duan, et al., J. Mater. Chem. A1 (2013) 12255-12262.
11. B. Zeng, X.H. Chen, X.T. Ning, et al., Catal. Commun. 43 (2014) 235-239.
12. D. Zhao and Z. Nan, Funct. Mater. Lett. 29 (2016) 1650009-1650013.
13. V.A. Smirnov, A.D. Mokrushin, V.P. Vasiliev, et al., Appl. Phys. A122 (2016) 513-521.
14. D. Das and R.K. Dutta. J. Colloid Interf. Sci. 457 (2015) 339-344.
15. B. Zeng and H. Long, Appl. Surf. Sci. 357 (2015) 439-444.
16. G.M. Zhang, Z.Y. Fu, Y.C. Wang, et al., Adv. Powder Technol. 26 (2016) 1183-1190.
17. J.H. Lu, X. Zhang, N.K. Liu, et al., J. Electroanal. Chem. 769 (2016) 21-27.